#6781

Building and Environment, Vol. 28, No. 2, pp. 201–210, 1993.
Printed in Great Britain.

0360-1323/93 $6.00 + 0.00
Pergamon Press Ltd.

Evaluating Models for Superposition of Wind and Stack Effect in Air Infiltration

I. S. WALKER
D. J. WILSON*

Models designed for routine calculations of air infiltration rates into buildings often use a semi-empirical function to combine the separately calculated wind-effect and stack-effect flow rates. The actual superposition of wind and buoyancy-generated pressure fields is a complicated non-linear process that is strongly influenced by the distribution of leakage sites on the building envelope. In the present study large sets of hourly-averaged air infiltration measurements using a constant concentration tracer gas injection system were sorted to separate stack-driven, wind-driven and wind-direction shelter effects. These data sets were then used to test superposition errors for linear, quadrature and flow coefficient methods for superposition of wind and stack effects. By using measured values of wind and stack dominated extremes, tests of the superposition methods were made independent of theoretical models for the wind-effect and stack-effect flows. The best superposition model was one using simple pressure addition. Results show that simple non-linear superposition models are an acceptable approximation to estimate average infiltration rates for combined wind and stack effect.

INTRODUCTION

CALCULATION of heating and cooling loads, and determination of fresh air ventilation rates require an estimate of the air infiltration rate through building envelopes. This natural ventilation by air infiltration depends on the size and location of air leakage sites on the building envelope and the indoor–outdoor pressure difference across each of these sites. These pressure differences are the result of a non-linear interaction between wind pressures on the exterior of the building and stack effect pressures caused by the density difference between indoor and outdoor air. These independent wind and stack effects interact to set the indoor pressure that maintains a balance between the overall infiltration and exfiltration mass flow rates.

Including both wind and stack effect pressures in an air infiltration model requires an iterative numerical solution of the flow balance to set an indoor pressure. Considering the uncertainty in estimating wind shelter and in determining the distribution of leakage sites, an exact solution of the combined wind and stack effect is often unjustified. The simplified models for air infiltration such as those of Sherman and Grimsrud [1], Warren and Webb [2], Shaw [3] and Walker and Wilson [4] yield closed-form approximations by calculating wind-effect and stack-effect infiltration separately, and then combining them in an empirical superposition equation.

Sherman [5] examined several of these superposition equations by comparing their predictions to exact solutions for combined wind and stack effects. He concluded that the accuracy of any empirical superposition function depends on the way in which leakage is distributed between walls, ceiling and floor, because the location of leakage on the envelope determines the wind and stack pressures that occur across each leakage site. In the present study we used measured air infiltration rates for wind-dominated and stack-dominated régimes in two test buildings to evaluate empirical relationships for superposition. By relying on a large data base of air infiltration measurements, the comparisons were independent of the pressure-flow relationship assumed in the models. The measured data sets also provided an indication of the variability in predicting air infiltration so that errors in superposition methods can be compared to other sources of uncertainty.

* Department of Mechanical Engineering, University of Alberta, Edmonton, Canada T6G 2G8. Address correspondence to D. J. Wilson.

PRESSURE AND FLOW RELATIONSHIPS

All the empirical superposition methods discussed here are based on the idea that it is physically more reasonable to add the wind and stack pressures than it is to add the flow rates. In fact, we will show later that adding the independent stack and wind effect solutions is strictly incorrect. Pressure addition methods require that some relation be specified for the averaged pressure-flow characteristics of the infiltrating leakage sites. Most infiltration models use a power law relationship between applied pressure difference ΔP across the envelope and the infiltration flow rate, Q in the form

$$Q = C\Delta P^n. \quad (1)$$

For orifice-type leaks such as holes in a vapour barrier we expect $n = 0.5$, and for long, narrow leakage channels the upper limit on n is the fully developed laminar flow condition $n = 1.0$. The values of the empirical flow coefficient C and the exponent n are usually determined from fan pressurization testing of the specific building in

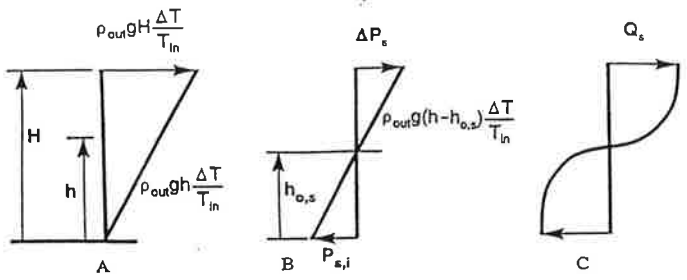

Fig. 1. Stack effect pressure and flow.

question or from the results of groups of similar buildings. Laboratory measurements by Shapiro *et al.* [6] of pressure drop in the developing flow of short laminar tubes suggest that $n = 0.67$ is a good approximation for a wide variety of leakage sites.

An alternate method for characterizing the pressure-flow relationship for leakage sites was suggested by Etheridge [7] who considered the pressure drop to be caused by orifice-type entrance and exit losses combined with fully developed laminar flow in each crack. By ignoring the developing flow (that may persist for 10 to 200 crack widths from the inlet) this approach yields

$$\Delta P = C_1 Q + C_2 Q^2, \tag{2}$$

where the quadratic term is the combined entrance and exit loss and the linear term is the fully developed laminar flow contribution.

Air infiltration models that deal with wind and stack effects independently use (1) or (2) to calculate the stack effect volume flow rate Q_s from the stack pressure difference ΔP_s caused by buoyancy,

$$\Delta P_s = f_s P_{stack}, \tag{3}$$

where f_s is the stack effect factor that accounts for the location of leakage sites and balance of inflows and outflows and P_{stack} is a characteristic pressure difference defined by

$$P_{stack} = \rho_{out} g H \frac{\Delta T}{T_{in}}, \tag{4}$$

where ρ_{out} (kg m^{-3}) is the outdoor air density at T_{out}, g (ms^{-2}) is the acceleration of gravity and ΔT is the indoor–outdoor temperature difference ($T_{in} - T_{out}$), (K), used to represent the fractional density difference of air ($\rho_{out} - \rho_{in})/\rho_{out}$ as $\Delta T/T_{in}$. The height H is the distance between the highest and lowest leakage sites on the envelope, usually the lowest above-grade floor level to the ceiling level.

STACK AND WIND-EFFECT PRESSURES

Figure 1A illustrates the linear change of stack pressure with height, h, given by

$$P_s(h) = \rho_{out} g h \frac{\Delta T}{T_{in}}. \tag{5}$$

where the maximum pressure is P_{stack} (i.e. at $h = H$). This figure is for the case when $T_{in} > T_{out}$. The sign of the pressure is reversed for $T_{out} > T_{in}$. In order to balance the flows in and out of the building there is a pressure shift, $P_{s,i}$, inside the building that results in the pressure variation shown in Fig. 1B. This produces outflow through the upper part of the wall and inflow in the lower part. At the neutral level height $h_{o,s}$, dependent upon the leakage distribution, there is no pressure difference across the wall. The pressure difference across the structure then varies linearly with height h,

$$\Delta P_s(h) = \rho_{out} g (h - h_{o,s}) \frac{\Delta T}{T_{in}}. \tag{6}$$

From Fig. 1A, the internal pressure shift $P_{s,i}$ is equal to the pressure at the neutral level height, $h_{o,s}$, before the flows were balanced.

$$P_{s,i} = -\rho_{out} g h_{o,s} \frac{\Delta T}{T_{in}}. \tag{7}$$

Thus the change in stack effect pressure with height, equation (6), may also be written as equation (5) minus equation (7):

$$\Delta P_s(h) = \rho_{out} g h \frac{\Delta T}{T_{in}} - P_{s,i}. \tag{8}$$

The flow resulting from this pressure distribution is illustrated in Fig. 1C.

In the same way, the wind effect volume flow rate Q_w is a function of ΔP_w,

$$\Delta P_w = f_w P_{wind}, \tag{9}$$

where f_w is the wind effect factor, dependent on leakage distribution, pressure coefficients (C_p) and the inflow and outflow balance, and P_{wind} is a characteristic dynamic pressure for windspeed, U,

$$P_{wind} = \frac{\rho_{out} U^2}{2}. \tag{10}$$

The outside wind pressure on one wall is shown in Fig. 2A. The pressure coefficients, C_p, for ventilation models

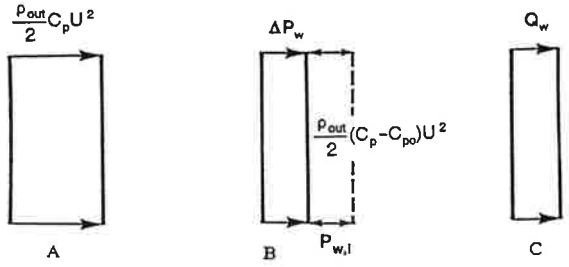

Fig. 2. Wind effect pressure and flow.

come from wind tunnel and full scale experiments where the external surface pressures are measured.

The pressure difference across the envelope is set by the internal pressure of the building that will balance total inflow and outflow summed over all leakage sites. The effect of the change in internal pressure, $P_{w,i}$, is shown in Fig. 2B. The wind pressure difference across the building envelope is given by

$$\Delta P_w = \frac{\rho_{out}}{2} C_p U^2 - P_{w,i}. \tag{11}$$

Here, the pressure shift is

$$P_{w,i} = -\frac{\rho_{out}}{2} C_{po} U^2, \tag{12}$$

where C_{po} is the internal pressure coefficient that balances inflows and outflows. Equation 11 can also be written in terms of pressure coefficients as

$$\Delta P_w = \frac{\rho_{out}}{2} (C_p - C_{po}) U^2. \tag{13}$$

EMPIRICAL SUPERPOSITION METHODS

Superposition methods rely on adding the independent stack and wind pressures as illustrated in Fig. 3A. The resulting flowrate, Q_{total}, shown in Fig. 3B is then calculated using a pressure-flow relationship. Instead of the zero pressure difference level being at $h_{o,s}$, the neutral level for stack effect only, it has been shifted to h_o due to the wind pressure. This neutral plane can be above or below the building depending on the contribution of wind effect. In the limiting case of no stack effect this plane is undefined.

Unfortunately the above method of adding pressures does not give the actual total pressure difference across the building envelope because ΔP_s and ΔP_w will usually have different internal pressures ($P_{s,i}$ and $P_{w,i}$). There can only be a single internal pressure for the building that results from the combination of stack and wind effects. This internal pressure balances the flows resulting from the addition of the individual wind and stack pressures in Figs 1A and 2A. The solution to this non-linear problem can only be found using iterative models. To avoid the use of complex iterative models several simple methods of superposing the stack and wind effects have been proposed, and this paper deals with the evaluation of these simple methods.

Four empirical superposition methods were tested in this study. A popular method used by Sherman and Grimsrud [1], Warren and Webb [2] and ASHRAE [8] is that of adding the stack (Q_s) and (Q_w) flowrates in quadrature. Adding independent stack and wind effect pressures, assuming orifice flow (i.e. Equation (1) with $n = 1/2$) to replace the pressure difference terms with flowrates, yields

$$Q_{total} = (Q_s^2 + Q_w^2)^{1/2}. \tag{14}$$

Another method is that of adding pressures used by Shaw [3] and Wilson and Pittman [9] for a variable n model, which by a similar analysis gives

$$Q_{total} = (Q_s^{1/n} + Q_w^{1/n})^n. \tag{15}$$

Equation (14) can be said to be a special case of equation (15) if orifice flow, with $n = 1/2$, is assumed.

Modera *et al.* [10] found that quadrature superposition tends to overestimate combined infiltration rates. Overprediction is greatest when stack and wind effects are equal; but when one or the other dominates the error is reduced. Some of this overprediction arises from the interaction between stack and wind effects through the internal pressure which both influence to balance inflow and outflow rates.

To account for this interaction an interference term can be introduced to act as a simple first order indoor pressure shift correction. This is the superposition method used by Walker and Wilson [4] in the Alberta Infiltration Model, AIM-2, and will be referred to as AIM-2 superposition, given by

$$Q_{total} = [Q_s^{1/n} + Q_w^{1/n} + B_1 (Q_s Q_w)^{1/2n}]^n, \tag{16}$$

where $B_1 (Q_s Q_w)^{1/2n}$ is the interaction term. By fitting equation (16) to measured data it has been found that $B_1 \cong -0.33$. The interference term disappears when either stack or wind effects dominate and has the greatest effect when they are equal. The form of the interference then is chosen to retain dimensional consistency, unlike some previously tested superposition methods, Lyberg [11]. Quadrature and AIM-2 superposition produce similar results because when $Q_w = Q_s$, equating the total flowrates in equations (14) and (16) results in $B_1 = (2^{(1/2n)} - 2)$. House pressurization test surveys by Sulatisky [12], Offerman *et al.* [13] and Dumont *et al.* [14] have shown that for a typical house, $n \simeq 2/3$, which result in $B_1 = -0.32$. This value of B_1 is close to the value of $-1/3$ chosen empirically for AIM-2 superposition.

The simplest method of combining Q_s and Q_w is to add them linearly

$$Q_{total} = Q_s + Q_w. \tag{17}$$

This method will produce large errors when the stack and wind effects are equal. For pressure addition when $Q_s = Q_w = Q$ the total flow rate is given by

$$Q_{total} = 2^n Q,$$

for linear addition the total flow rate is given by

$$Q_{total} = 2Q,$$

and linear addition will overpredict by a factor of 2^{1-n}. With $n = 2/3$ this is an overprediction of 26%. Despite the expected overprediction of total flow this method has been included for comparison to the other methods.

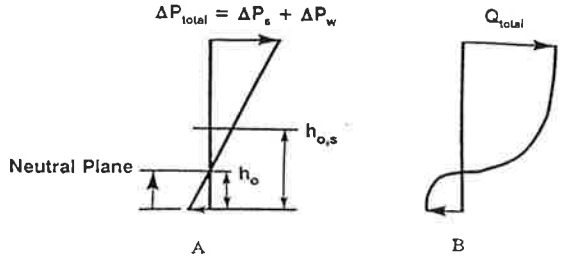

Fig. 3. Total pressure difference and flow rate resulting from addition of wind and stack pressures.

Another method of characterizing the pressure-flow relationship for a building envelope, rather than the power law equation (1), is to use a quadratic with a linear term for laminar flow contribution and a squared term for turbulent flow contribution Etheridge [7] given by equation (2). This equation may be used as the pressure-flow relationship for ΔP_{total} and Q_{total}, ΔP_s and Q_s, and ΔP_w and Q_w. Adding the relationships for stack and wind effect and equating the result to the total flow results in the quadratic relationship

$$Q_{total} = \left[\left(\frac{r}{2}\right)^2 + r(Q_w + Q_s) + Q_w^2 + Q_s^2\right]^{1/2} - \frac{r}{2}, \quad (20)$$

where r is the ratio of flow resistance coefficients C_1 and C_2 in equation (2):

$$r = \frac{C_1}{C_2}. \quad (21)$$

For fully developed turbulent flow $r = 0$. As the fully developed laminar flow limit is approached, $C_2 \to 0$ and r becomes undefined. However, using equation (2) it can be shown that in the limit where $C_2 = 0$ equation (20) applies, with $r = 1$.

In the present study, fan pressurization tests were used to determine C and n in equation (1). By equating the flow rates at any two pressures the constants C_1 and C_2 in equation (2) may be found from the C and n in equation (1). The two reference pressure differences chosen here are $\Delta P = 1.0$ and 10.0 Pa because pressures across building envelopes due to stack and wind effects usually fall in this range. Using these two reference pressures in equations (1) and (2), r can be expressed in terms of C and n as

$$r = \frac{C(1 - 10^{2n-1})}{(10^{n-1} - 1)}. \quad (22)$$

TEST SITE DESCRIPTION

The Alberta Home Heating Research Facility is made up of six permanent test houses with poured concrete basements. The six unoccupied test houses have been continuously monitored since 1980 for building envelope energy losses and air infiltration and ventilation rates.

The flat exposed test site is located on rural farm land, with fields planted in forage and cereal crops in summer, becoming snow-covered stubble in winter. Windbreaks of mixed poplar and spruce trees cross the landscape at intervals of a few kilometres. One of these windbreak rows with 20 metre high trees is located parallel to the line of the houses about 250 m to the north, and another windbreak lies 100 m to the northeast. A row of 3 metre high trees runs perpendicular to the line of the buildings to the southwest. The houses are totally exposed to south and east winds. Wind shelter from man-made structures is dominated by two-storey storage and machinery buildings located about 50 m to the northeast.

The houses are situated in a closely-spaced, east-west line with about 2.6 m separation between their side walls. False end walls, with a height of 3.7 m but without roof gable peaks, were constructed beside the end houses of the line to provide wind shelter and solar shading similar to that experienced by interior houses in the row. The distributed background envelope leakage, that does not include any intentional openings such as furnace flues, is found from fan pressurization tests. The results of these tests are shown in Table 1.

House #1 has double wall construction with foamed-in-place urethane insulation between an inner concrete block wall and an outer wall of clay brick. The foamed-in-place insulation provides a tight seal around 5 windows, one door, 13 electrical conduit pipes, and along the top of the basement wall. The inside of the concrete block wall has 8 surface mounted electrical outlet boxes. The major ceiling leakage sites consist of electrical conduit penetrations for 3 fluorescent light fixtures, and a 1 cm wide annular crack around the 20 cm O.D. (15.2 cm I.D.) flue pipe.

House #5 is constructed to typical 1980 Canadian residential housing standards. The 2×4 wood frame walls are insulated with fibreglass batts, with a polyethylene air-vapour barrier behind the gypsum board interior walls and ceiling. The only unconventional construction detail is that the air-vapour barrier is passed under the floor of the wood frame wall, and carried down over the joists to seal the crack at the top of the concrete basement wall. The box surrounding the floor joists has 7 penetrations for electrical conduit pipes and a sump drain pipe. The vapour barrier has 8 interior penetrations for electrical boxes in the walls, and 3 electrical boxes in the ceiling to serve the fluorescent light fixtures. The major ceiling leakage site is a 1 cm wide circular crack around the 20 cm O.D. flue pipe as it passes through the ceiling. For the tests performed here the furnace flue was sealed.

In addition to having a smaller floor area, the test modules differ from a standard house in that they have no plumbing or sewer drains, and no interior partition walls except for an entryway with an open interior doorway. The absence of interior walls promotes air mixing, and allows the house to be treated as a single air exchange zone. The houses are heated electrically with a centrifugal

Table 1. Distributed background envelope leakage from fan pressurization tests with flue sealed, windows closed $Q = C(\Delta P)^n$

	Pressurization			Depressurization		
House	Flow coefficient C $m^3/(s \cdot Pa^n)$	Flow exponent n	Leakage area A_L cm^2 at 4 Pa	Flow coefficient C $m^3/(s \cdot Pa^n)$	Flow exponent n	Leakage area A_L cm^2 at 4 Pa
1—Masonry	0.00250	0.763	27.9	0.00274	0.740	29.6
5—Reference	0.00937	0.625	86.3	0.00970	0.661	93.6

fan distributing air through under-floor ducts to the main-floor room. The fan in the electric heater operates continuously, recirculating 4.5 house interior volumes per hour to ensure complete mixing of air infiltration with indoor air tagged with SF_6 tracer gas. Air from the upstairs outlets returns to the basement through the large open stairwell. To avoid basement air stratification, a fan intake is located near the basement floor, and another intake is close to the ceiling.

A thermostat located on the room side of the entryway wall maintained the interior temperature at 22°C ± 0.5°C during the heating season. In summer, the fan circulated through the house, and the room temperature was governed by ventilation and heat gains through the walls and windows. Summer indoor temperature rarely differed by more than ±5°C from the outdoor air.

AIR EXCHANGE MEASUREMENTS

Air infiltration rates were measured using a tracer gas system that injected sulphur hexafluoride, SF_6, to maintain a constant concentration in each of the test houses. The total volume of tracer gas, injected eight times each hour, is proportional to the amount of outside air that enters the house and is brought up to the 5.0 ppm setpoint. The gradual decrease of concentration in each of the 7.5 min periods between injections was accounted for in the data analysis to determine a true hourly average concentration, typically 4.8 ppm. The calibration and operating techniques applied to the gas analyzers is described in more detail in Wilson and Walker [15].

Measurement uncertainty was much smaller than the hour-to-hour natural variability of air infiltration rate. An uncertainty analysis of the injection and concentration measuring systems indicated that the standard deviation in measured infiltration rate was ±2.5% of the air exchange rate, added to an absolute error of ±0.0025 ACH. This corresponds to a standard deviation of about ±3% at typical air exchange rate of 0.3 ACH. For random variations this implies a range of about ±6% to encompass 95% of data scatter due to measurement uncertainty.

The wind speed and direction at 10 m height was measured at a distance of about 12 m from the buildings with a low-friction cup anemometer and rotating direction vane. Wind speeds and directions were measured at 2.5 minute intervals and averaged hourly. Both the mean and standard deviation of these 24 readings for wind speed and direction were recorded. In addition, east and north vector components of each of the 24 readings were calculated. and stored as mean-squared averages over the hour. These mean-square values were then used to compute the standard deviation of wind speed, and to calculate a true average wind-run direction.

CORRECTING MEASUREMENTS FOR WIND AND STACK EFFECT INTERACTION

To examine the effectiveness of the superposition techniques, Q_s and Q_w were estimated from measured data rather than using a model, since errors in the model predictions may mask the behaviour of the superposition. The same measured data used to predict Q_s and Q_w was used in the superposition testing.

To estimate Q_s data sets were sorted to remove points with $U > 1.5$ m/s. At these low windspeeds the measured ventilation rate is dominated by stack effect. This low windspeed data is shown in Fig. 4 for house # 1 with a 15 cm I.D. flue. Data scatter in Fig. 4 is caused by averaging infiltration rates and windspeeds over hourly periods, and by residual wind effects. To show data trends more clearly the data was sorted into bins 5°C wide. The mean and standard deviation of the data in each bin is calculated and shown in Fig. 5 where the error bars represent plus and minus one standard deviation.

The binning process also allowed for a direct correction for residual wind effect. The points in each 5°C wide ΔT bin were correlated to find any windspeed effect within each narrow ΔT range. Figure 6 shows the data points in the bin from 5°C to 10°C, with a mean of 7.8°C. Ideally with no wind effect there would be no trend in this data, but the air infiltration rate increases with windspeed. The true zero windspeed ventilation rate, i.e. Q_s only, is given by the ventilation rate at $U = 0$ and must be estimated because the measured windspeed is never exactly zero. The $U = 0$ intercept of a linear least square fit to the data in each bin was used as the best estimate of the true stack-effect flow Q_s. A linear fit was used as it is the simplest method of determining the $U = 0$ intercept. Use of more complex methods (e.g. a power law) cannot be justified due to the amount of scatter in the data. The scatter is mainly due to the use of hourly averaging of the data where changes in wind direction during the hour can cause significant changes in ventilation rate. In this case, the zero windspeed intercept was 0.013 ACH, and the mean value of all the points in this bin was 0.033 ACH. The windspeed effect on these data acted to increase the mean ventilation rate by a factor of about 2.5. For other bins of data at higher temperature differences the change in ventilation rates is typically 10% or less. The data set illustrated in Fig. 6 is presented here as it clearly shows the residual wind effect that is being corrected for. For bins of data with few points the least squares fit line sometimes produced unrealistic estimates, in which case the zero windspeed infiltration rate was estimated by inspection and was usually taken to be the average of the data. Since these corrections are small it is reasonable to use no correction for bins of data with a few highly scattered data points.

The results of removing windspeed effects can be seen by comparing Fig. 5 to Fig. 7 where the mean value of each bin has been adjusted to its zero windspeed intercept. The changes have greater effect at lower ΔT's where the wind has the gratest relative effect. To find Q_s for any ΔT a linear interpolation is performed between the zero windspeed adjusted mean of each bin.

To estimate wind effect, the data was sorted for low temperature differences $\Delta T = \pm 10$°C. Wilson and Walker [15] have shown that wind direction and shelter effects have a large influence on ventilation rates therefore only winds from a single direction are chosen. At the test site prevailing winds tend to be from the south, so to maximize the quantity of valid data wind directions of 180° ± 22.5 were used i.e. a bin 45° wide centred on south (180°). The same binning procedure and adjustment to

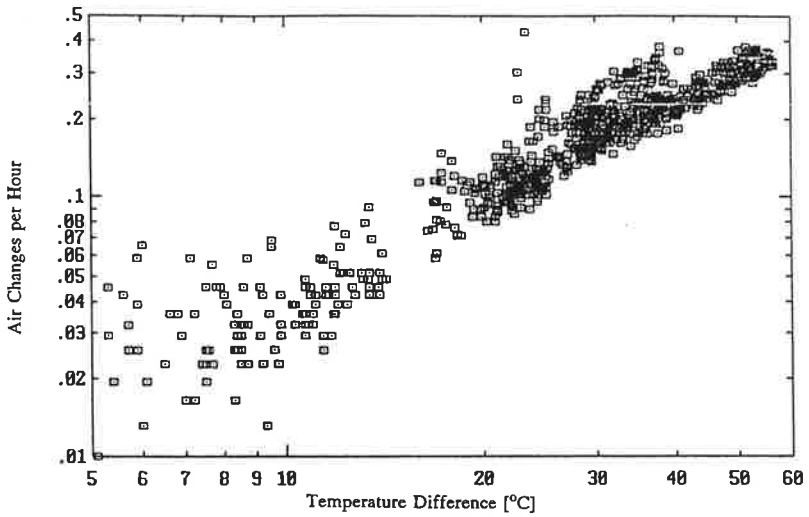

Fig. 4. Stack effect dominated infiltration rates (ACH) for house #1 with a 15 cm I.D. furnace flue: $U < 1.5$ m/s and $5°C < \Delta T < 60°C$ (847 hours).

zero temperature difference was followed for wind effect to find Q_w at each bin averaged windspeed U. The size of the corrections were smaller than those for the temperature bins, with the largest correction being about 25% at low windspeeds and dropping to a couple of percent above 3 m/s. Linear interpolation between adjusted windspeed bins was used to recover the measured Q_w vs. U relationship.

Superposition testing

With Q_s and Q_w estimated directly from the measured data, superposition methods can be evaluated without the results being contaminated by effects of modelling. The relative contribution of wind and stack effect to the total flowrate is determined by the ratio Q_w/Q_s. To remove the dependence of this ratio on building leakage distribution an appropriate non-dimensional ratio is that of the characteristic pressures for wind and stack effect, from equations (4) and (10)

$$\frac{P_{wind}}{P_{stack}} = \frac{U^2 T_{in}}{2gH\Delta T}. \tag{23}$$

The four superposition techniques analyzed here are:

(1) Quadrature addition of flowrates, equation (14).
(2) Pressure addition, equation (15).
(3) Pressure addition with an interaction term (AIM-2 superposition), equation (16).
(4) Linear addition of flowrates, equation (17).

The data sets used to estimate Q_s and Q_w were combined, and for each data point the ratio of the total ventilation rate predicted by superposition to the measured ventilation rate, $Q_{total}/Q_{measured}$ and the ratio P_{wind}/P_{stack} was

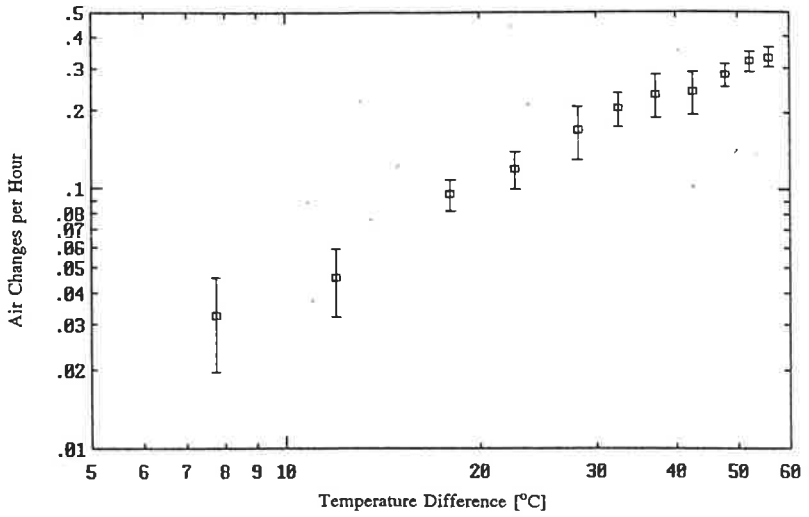

Fig. 5. Binned infiltration rates (ACH) for house #1 with a 15 cm I.D. furnace flue: $U < 1.5$ m/s and $5°C < \Delta T < 60°C$ (847 hours).

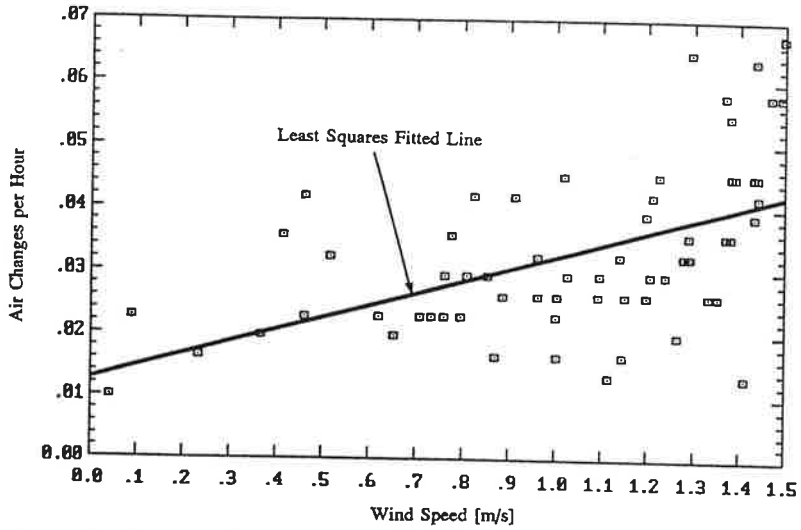

Fig. 6. Windspeed effects on infiltration in house #1 for $U < 1.5$ m/s and for a single ΔT bin: $5°C < \Delta T < 10°C$.

found for each superposition method. For clarity, the mean and standard deviation of $Q_{total}/Q_{measured}$ was binned. Figure 8 shows results for house #1, with approximately 75% of the total building leakage area in the furnace flue. This highly nonuniform leakage distribution was chosen to reveal the shortcomings of the four simple superposition equations, none of which include leakage distribution parameters. For the 950 hours in this data set, the ratio P_{wind}/P_{stack} covers a large range of 5 orders of magnitude. At the extremes of stack or wind dominated flow the errors are minimalized since we have empirically determined Q_s and Q_w from the measured data. The maximum error of 35% (0.014 ACH) was produced by linear flow superposition when stack and wind characteristic pressures were approximately equal. A similar result was found by Modera *et al.* [10] using quadrature superposition and the LBL orifice flow infiltration model from Sherman and Grimsrud [1], where the greatest overprediction of total flowrate occurred when stack and wind flows were approximately equal. Figure 8 shows that quadrature does not necessarily produce an overprediction if Q_s and Q_w are estimated correctly. Errors due to overprediction of low flowrates by the LBL model manifest themselves in overprediction of combined flowrates when the flows are about equal, which usually occurs when both flowrates are low. Apart from linear addition the other three methods produce results for house #1 that are within 10% of each other, with pressure addition producing the smallest errors. All underpredict by up to 15% for some ranges of P_{wind}/P_{stack}.

To further test these superposition techniques the same analysis techniques were applied to 541 hours of data from house #5, which had no furnace flue and a relatively uniform distribution of leakage sites. The results are shown in Fig. 9 where, as in Fig. 8, linear addition

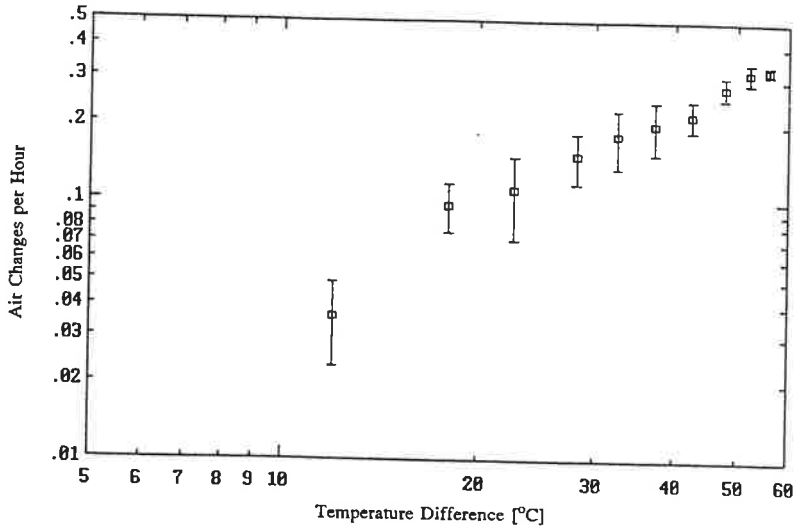

Fig. 7. Binned infiltration rates in house #1 with mean value of each bin adjusted to the zero windspeed intercept.

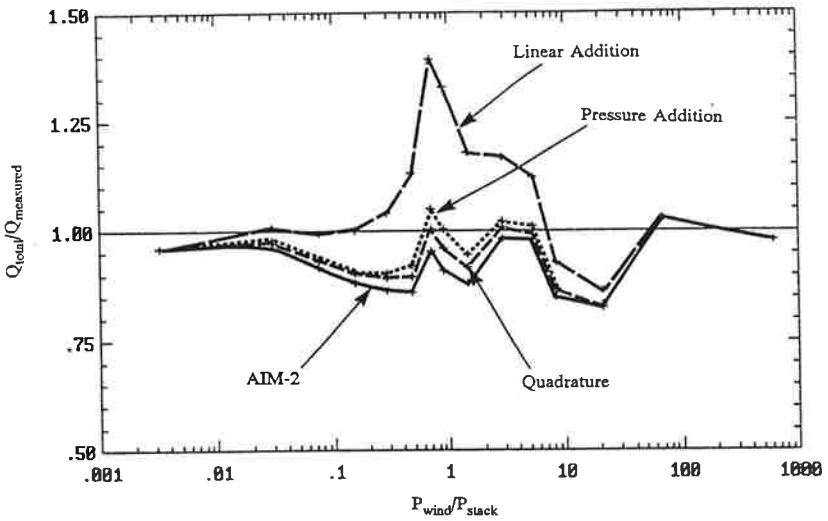

Fig. 8. Superposition errors for house #1 with 15 cm I.D. furnace flue (950 hours).

produces the greatest error, up to 48% (0.04 ACH) when wind and stack pressures are about equal. The other three models are within 10% of each other. Pressure addition produced the greatest error of the three, with an over-prediction of 18% (0.02 ACH) when $P_{wind}/P_{stack} \simeq 8.4$.

Figure 10 shows the points for pressure addition with error bars indicating ± 1 standard deviation of $Q_{total}/Q_{measured}$ in each bin. This indicates the amount of uncertainty associated with this analysis, with one standard deviation being typically 25%. This magnitude of uncertainty is similar for all the models, and for both the buildings tested. Given this uncertainty it is difficult to choose one of the three methods of non-linear superposition over the others. Pressure addition is the simplest physically realistic method tested, and is recommended because its performance is not significantly bettered by pressure addition with an interaction term, or by quadrature, which is physically unrealistic except in the case of orifice flow.

Etheridge's equation applied as pressure addition (equation (20)), is compared to power law pressure addition in Fig. 11. As expected the two produce almost identical results especially in view of the uncertainty represented by the measurement uncertainty shown in the figure as one standard deviation error bars.

SUMMARY AND CONCLUSIONS

A large data base of 1491 hours of constant concentration tracer gas air infiltration measurements has been used to evaluate superposition of wind and stack induced flowrates. The data was taken in two houses, chosen for their different leakage distributions, at the Alberta Home Heating Research Facility in Edmonton, Canada. Estimates of the stack effect and wind effect flow rates were based on adjusted correlations from the measured data. Linear addition is physically incorrect (but included here for its simplicity) and produces the

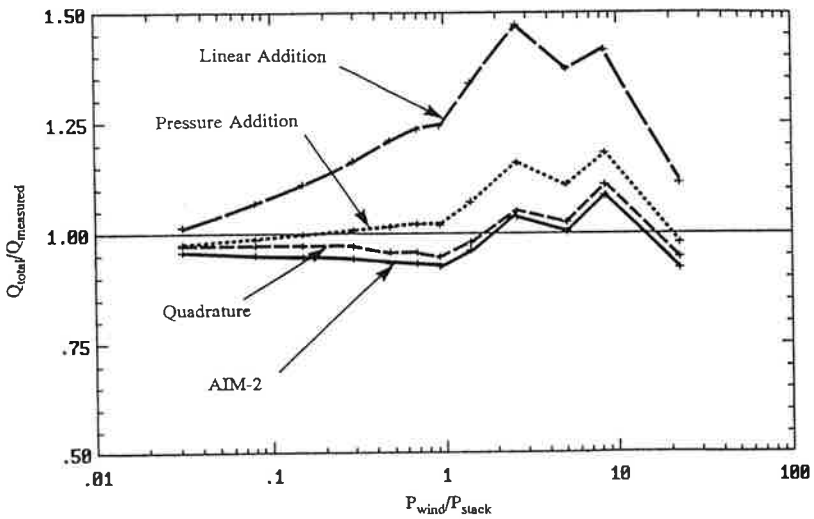

Fig. 9. Superposition errors for house #5 with no furnace flue (541 hours).

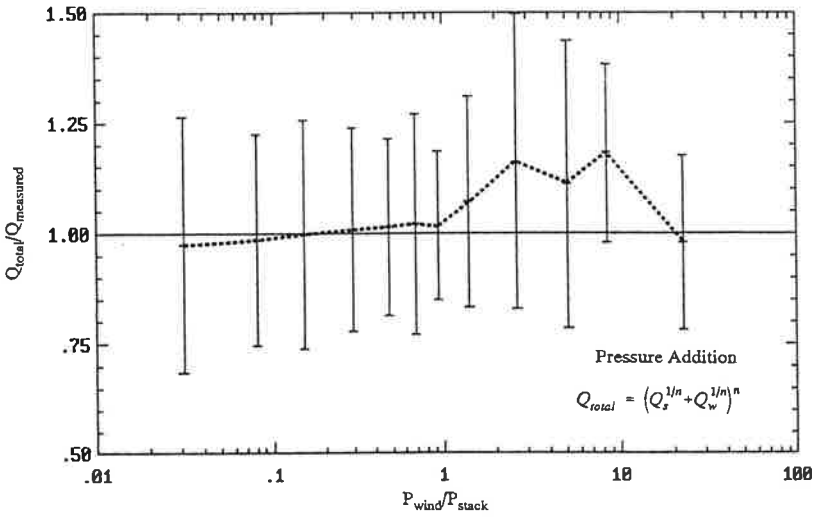

Fig. 10. Pressure addition superposition with error bars showing ± 1 standard deviation for house #5 with no furnace flue (541 hours).

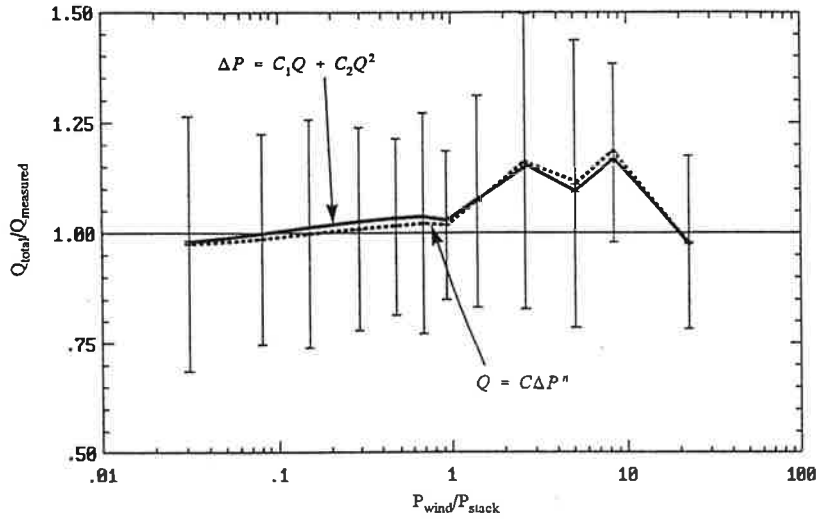

Fig. 11. Comparison of pressure addition superposition using two different pressure-flow relationships in house #5 (541 hours).

greatest errors of up to 50%. The other three non-linear models are more physically realistic, and produce maximum errors of about 10%.

Simple pressure addition, equation (15) does not account for the interaction of wind and stack effect through a shift in the neutral pressure level $h_{o,s}$ to h_o. In spite of this deficiency, equation (15) appears to work as well as the AIM-2 superposition, and the physically unrealistic quadrature equation. Because pressure addition is physically realistic, simple, and has errors less than the hour to hour natural variability of measured infiltration, this method seems to be the best choice for combining independent wind effect and stack effect flows to estimate their combined effect.

REFERENCES

1. M. H. Sherman and D. T. Grimsrud, Measurement of Infiltration using Fan Pressurization and Weather data, Lawrence Berkeley Laboratories Report Number 10852, University of California (1980).
2. P. R. Warren and B. C. Webb, The Relationship Between Tracer Gas and Pressurization Techniques in Dwellings, *Proc. First Air Infiltration Centre Conference*, pp. 245–276 (1980).
3. C. Y. Shaw, Methods for Estimating Air Change Rates and Sizing Mechanical Ventilation Systems for Houses, Building Research Note 237, Division of Building Research, National Research Council of Canada (1985).

4. I. S. Walker and D. J. Wilson, AIM-2: The Alberta Air Infiltration Model, Department of Mechanical Engineering Report 71, University of Alberta (1990).
5. M. H. Sherman, Superposition in Infiltration Modelling, *Indoor Air 2*, 101–114 (1992).
6. A. H. Shapiro, R. Siegel and S. J. Klein, Friction Factor in the Laminar Entry Region of a Smooth Tube, *Proc. Second U.S. National Congress of Applied Mechanics*, American Society of Mechanical Engineers (1954).
7. D. W. Etheridge, Crack Flow Equations and Scale Effect, *Bldg Envir.* **12**, 181–189 (1977).
8. ASHRAE Fundamentals Handbook, Chapter 22. American Society of Heating Refrigerating and Air Conditioning Engineers, Atlanta, Georgia (1989).
9. D. J. Wilson and W. Pittman, Correlating Measured Infiltration for Wind from a Single Direction, *ASHRAE Trans.* **89**, part 2B, 211–227 (1983).
10. M. Modera, M. H. Sherman and P. S. Levin, A Detailed Examination of the LBL Infiltration Model Using the Mobile Infiltration Test Unit, Report No. LBL-15646, Lawrence Berkeley Laboratories, University of California (1983).
11. M. D. Lyberg, Models of Infiltration and Natural Ventilation, Bulletin M83:23, National Swedish Institute for Building Research (1983).
12. M. Sulatiski, Airtightness Tests on 200 New Houses Across Canada: Summary of Results, Buildings Energy Technology Transfer Program, Publication No. 84.01, Energy Mines and Resources Canada (1984).
13. F. J. Offerman *et al.*, Residential Air Leakage and Indoor Air Quality in Rochester, New York, Lawrence Berkeley Laboratory Report 13100 (1982).
14. R. S. Dumont *et al.*, Air Tightness Meaurements of Detached Houses in the Saskatoon Area, Building Research Note No. 178, National Research Council of Canada (1981).
15. D. J. Wilson and I. S. Walker, Passive Ventilation to Maintain Indoor Air Quality, Dept. of Mechanical Engineering Report 81, University of Alberta (1991).